CORROSION SCIENCE AND TECHNOLOGY, Vol.3, No.4(2004), pp.131~139

Effects of PbO on the Repassivation Kinetics of Alloy 690

SeJin Ahn, HyukSang Kwon, JaeHun Lee*, YunWon Park*, and UhChul Kim**

Korea Advanced Institute of Science and Technology
**Korea Institute of Nuclear Safety*
***Korea Atomic Energy Research Institute*

Effects of PbO on the repassivation kinetics and characteristics of passive film of Alloy 690 were examined to elucidate the influences of PbO on the SCC resistance of that alloy. The repassivation kinetics of the alloy was analyzed in terms of the current density flowing from the scratch, *i(t)*, as a function of the charge density that has flowed from the scratch, *q(t)*. Repassivation on the scratched surface of the alloy occurred in two kinetically different processes; passive film initially nucleated and grew according to the place exchange model in which log *i(t)* is linearly proportional to *q(t)*, and then grew according to the high field ion conduction model in which log *i(t)* is linearly proportional to *1/q(t)* with a slope of *cBV*. The *cBV* is found to be a parameter representing repassivation rate and hence SCC susceptibility of the alloy. The lower the value of *cBV*, the faster the repassivation rate and the higher the SCC resistance of an alloy. Addition of PbO to pH 4 and 10 solutions increased the value of *cBV* of alloy 690, reflecting slower repassivation rate than without PbO. The change in the value of *cBV* was grater in pH 10 than in pH 4. The increase in SCC susceptibility of alloy 690 with the addition of PbO to solution was presumably due to the Cr-depletion in the outer parts of passive film of the alloy with an incorporation of Pb compounds in the film, which was revealed by Mott-Schottky, AES and XPS analyses.

Keywords *: alloy 690, repassivation, scratching electrode test, SCC, PbO*

1. Introduction

Alloy 600, widely used as a heat exchanger tube material in nuclear power plants, has experienced intergranular stress corrosion cracking (IGSCC) and intergranular attack(IGA) from either the primary side or the secondary side of steam generators. From the recognition that it is necessary to increase Cr contents in Alloy 600 to enhance the IGSCC resistance, Alloy 690, with chemical compositions of Ni-30Cr-10Fe, was developed and now replaced alloy 600 for stream generator tube.

It has been known that SCC of Alloy 600 and Alloy 690 in secondary side of steam generators occurs mainly in high a temperature caustic solution or in S containing solutions such as $H_2S_xO_6$ and Na_2S_2O. However, lead is now being considered as a new origin of SCC of Alloy 600 and Alloy 690. In the secondary sides of more than 30 nuclear power plants, worldwide, lead compounds has been detected.[1)-4)] Although there have been a few reports on lead-induced SCC of these alloys including the effects of alloying elements, micro-structure and lead chemicals on SCC resistance,[5)-7)] the mechanism of lead-induced SCC of Ni-based alloy is not yet well elucidated.

According to the film rupture/slip dissolution model which is considered to well explain the SCC of austenitic alloy including Alloy 600 and Alloy 690, the crack grows by a repetitive processes of film rupture/metal dissolution/repassivation.[8)] The repassivation is a film reforming process on the film broken surface, and hence its kinetics has been considered to be a critical factor in determining the susceptibility to SCC of an alloy.[8)] Thus, it is necessary to investigate the effects of lead on the repassivation kinetics of these alloys to elucidate why lead decreases the resistance to SCC of alloy 690.

The objective of this study is to investigate the mechanism of lead-induced SCC of Alloy 690, now being used as a steam generator tubing materials for new power plants, by examining the effects of lead on the repassivation kinetics and, further, on the properties of passive film which is known as an origin of high corrosion resistance of this alloy.

2. Repassivation kinetics

Most studies on the growth kinetics of passive film have been concentrated mainly on stainless steels. There have been few reports on growth kinetics of passive film on Ni-based alloys. So it is necessary to review growth

kinetics of passive film on stainless steels and to confirm the applicability of it to that on Ni-based alloys.

Formation of passive film on stainless steels is usually described by the models based on the pioneering works of Sato and Cohen[9] and Cabrera and Mott.[10] According to the place exchange model proposed by Sato and Cohen,[9] a layer of oxygen is adsorbed onto the surface and then exchanges places (possibly by rotation) with underlying metal atoms. A second layer of oxygen is adsorbed and the two M-O pairs rotate simultaneously. This process is repeated and results in the formation of oxide film. Based on this model, it was induced that logarithms of anodic current density ($i(t)$) are linearly proportional to charge density ($q(t)$) that has flowed from the scratch during repassivation;

$$\log i(t) = \log k' + \beta V - \frac{q(t)}{K} \quad (1)$$

where, k' and K are constants, V is the applied potential and $q(t)$ is experimentally determined by integration of the current density with time during the repassivation. On the other hand, according to the high field ion conduction model,[10] the passive film grows by the transport of metal ions across the film toward the film/electrolyte interface under high electric fields of a few MV/cm, and thus, the ion conduction rate through the film during repassivation is expressed by the current represented by Eq. (2);[10]

$$i(t) = A \exp[BV/h(t)] \quad (2)$$

where A and B are parameters associated with the activation energy for mobile ion migration, V is the potential drop across the film whose thickness is $h(t)$.

The anodic current measured on the scratched surface during repassivation is presumed to be consumed for two anodic processes; one is metal dissolution reaction, and the other is repassivation that is an oxidation reaction of metal with water to form the passive film. Burstein and Marshall[11] clearly demonstrated that for stainless steels in chloride solution, the anodic current measured during repassivation is mostly consumed to form passive film on the scratched surface as far as the metal dissolution does not become dominant by pitting or general corrosion, and hence the anodic current associated with the metal dissolution is negligibly small. Thus, by neglecting the current associated with the metal dissolution, the charge density ($q(t)$) that has flowed from the scratch during repassivation has the following relationship with the film thickness ($h(t)$);

$$q(t) = \frac{zF\rho}{M} h(t) \quad (3)$$

where z is the number of electrons transferred for an ion, F is the Faraday constant, ρ is the film density, and M is the molecular mass of film.

Combining Eq. (2) and (3) yields Eq. (4);

$$\log i(t) = \log A + \frac{BVzF\rho}{2.3Mq(t)} = \log A + \frac{cBV}{q(t)} \quad (4)$$

According to Eq. 4, $\log i(t)$ is linearly proportional to the $1/q(t)$ with the slope of cBV, where the c is a constant equal to $zF\rho / 2.3M$. Kwon et al.[12] reported that the value of cBV could be used as a parameter representing the repassivation rate and the SCC susceptibility of an alloy. The lower the value of cBV, the faster the repassivation rate and the higher the SCC resistance of an alloy.[12] As mentioned above, these models for growth kinetics of passive film is about that on stainless steels. If the repassivation reaction of Ni-based alloy (Alloy 690) occurs by the two models mentioned above, then the effects of PbO on the SCC susceptibility of Alloy 690 can presumably be examined in terms of the value of cBV.

3. Experimental

Alloy 690, used in this study provided by Sandvik company was a sleeve pipe 1.09 mm thick and 19.05 mm outside diameter. Specimens were machined into sheet form from the tubes. Table 1 shows the chemical compositions of the alloy used. All samples were given an isothermal solution anneal at 1150 ℃ for 1 hour, followed by a water quench. And then, the sensitization treatment was given to all specimens at 700 ℃ for 15 hours. This sensitization treatment, called TT (thermally treated), is known to cause the precipitation of semi-continuous Cr-carbide on the grain-boundaries of this alloy and to increase the SCC resistance.

Scratch tests were performed in 90 ℃, pH 4 and pH 10 water. Lead was added to the test solutions in the form of PbO with different concentration, 0 and 500 ppm. All the solutions were deaerated by purging with high-purity nitrogen throughout the test.

Table 1. Chemical compositions of Alloy 690 used in this study (wt%).

	C	Si	Mn	S	Al	Co	Cr	Cu	Fe	Ni	Ti
wt %	0.014	0.28	0.26	0.003	0.02	0.01	30.43	0.03	9.54	59.18	0.20

A cell was devised to measure repassivation current using a scratch electrode technique. The cell consisted of a specimen as a working electrode, a platinum counter electrode, a saturated calomel electrode (SCE) positioned in a salt bridge with a high silica tip, and a scratcher with an alumina tip. To rupture the surface film by making a scratch, an alumina tip loaded on a spring was pulled rapidly up along the surface of the specimen fixed into the specimen holder by an air pressure cylinder connected to a solenoid valve. The contact time of the alumina tip with the surface of the specimen during scratching was < 1 μs. Schematics of the cell was explained in detail in the previous paper.[13] Specimens were spot welded for electrical contact, cold-mounted in epoxy resin with exposed area of 0.6×10 mm^2 and surface finished to #2000 grit SiC paper. To prevent crevice corrosion, specimen edge contacted with epoxy resin was sealed by silicon sealant. Scratches were made potentiostatically after stable passive film was formed under the applied potential in the stable passive range for 30 minutes. Current was measured every msec and current density was calculated assuming that anodic reaction occurred only at the scratched region. In this experiment, contact time between specimen and tip was below 1 msec and resultant scratches had comparative uniform size, 35 μm in width and 0.6 mm in length.

The passive behavior of the alloy was examined using anodic polarization test conducted at a scan rate of 0.5 mV/s. Anodic polarization test was conducted in the same solutions in the case of scratch tests, 90 ℃, pH 4 and pH 10 water, after a stable corrosion potential (E_{corr}) had been achieved.

The effects of PbO on the semi-conducting properties of passive film formed on alloy 690 for 2 hours at the applied potential, determined from anodic polarization test, were examined by the Mott-Schottky analysis at a frequency of 1000 Hz, sweeping the applied potential in negative direction from 0.5 V_{SCE} to -1 V_{SCE} with excitation voltage of 10 mV (peak-to-peak) using a Frequency Response Analyzer. The imaginary part of the impedance (Z") was measured as a function of the applied potential, and the corresponding capacitance of space charge layer (C_{SC}) was obtained from $C_{SC} = -1/Z''$.

AES and XPS analyses for the passive film on alloy 690 were conducted to investigate the effects of PbO on the compositions of passive film on Alloy 690. The procedures for film formation were same as those for Mott-Schottky analysis. After film formation, the samples were rinsed with distilled water and stored in a desiccator. AES analysis was performed with 90 degree of take-off angle. Sputtering rate of argon ion was 1.6 Å/s calibrated with SiO_2. XPS analysis was performed with Al Kα (1486.6 eV).

4. Results and discussion

4.1 Anodic polarization curves

Fig. 1 shows anodic polarization curves of alloy 690 in pH 4(a) and pH 10(b) solutions, respectively at 90 ℃. In pH 4 solution, PbO addition to the solution caused a decrease in corrosion potential of the alloy by about 100 mV, and an increase in anodic current density, reflecting that PbO decreased the protectiveness of passive film. In pH 10 solution, anodic current density of alloy 690 increased in solution with PbO, but there was no change in corrosion potential. An interesting point in Fig. 1(b) is that the potential where anodic current peak appears is lowered by addition of PbO to the solution (peak 1 at 328 mV_{SCE} → peak 2 at 249 mV_{SCE}). It was reported

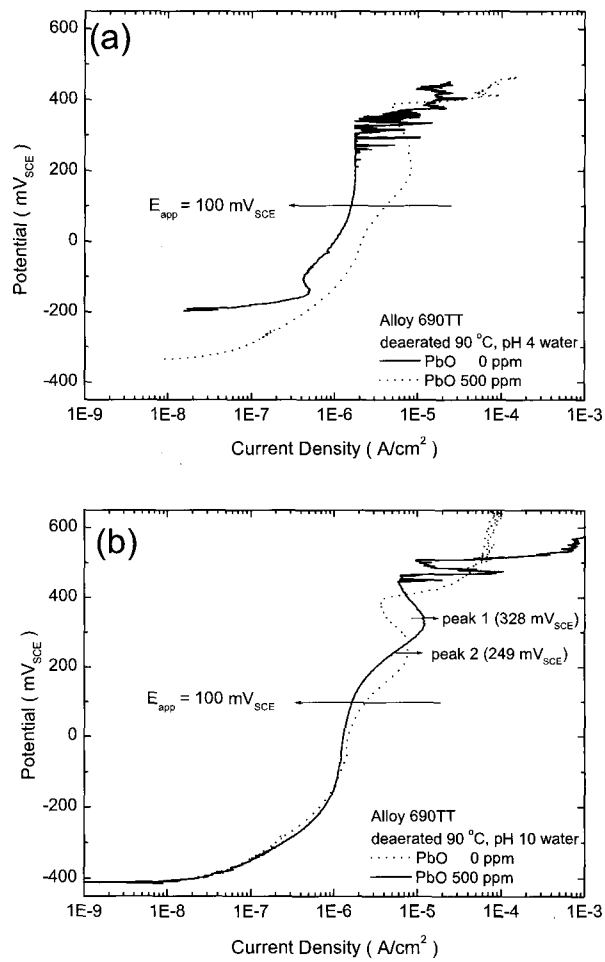

Fig. 1. Effects of PbO on the polarization behavior of Alloy 690 in deaerated 90 ℃, pH 4(a) and pH 10(b) solutions.

that in the polarization curves of alloy 600, the anodic current peak was caused by trans-passive reaction of Cr.[14] From Fig. 1(b), therefore, it appears that PbO addition to pH 10 solution makes it easy the dissolution of Cr in the passive film on alloy 690 by lowering trans-passive potential of Cr in the alloy. A potential value of 100 V_{SCE}, representing stable passive behavior of passive film in both solutions, was chosen as a film formation potential for further experiments.

4.2 SEM morphologies of passive film

Fig. 2 and Fig. 3 show SEM micrographs of passive film formed on alloy 690 in pH 4 and pH 10 solution, respectively, with 500 ppm of PbO for 2 hours at 100 mV_{SCE}. On the surface of passive film, lead-rich precipitates were formed as confirmed by EDS spectra, in Fig. 2(b) and Fig. 3(b). The number of precipitates on the passive film formed in PbO containing pH 10 solution were much more than that on film formed in pH 4 solution containing PbO. Feron et al.[15] reported that thermodynamically PbO could oxidize Ni, Cr and Fe by the following reactions.

$$M + PbO = MO + Pb \quad (5)$$

E^0 (Pb^{2+}/Pb) = -0.126 V_{SHE}
E^0 (Ni^{2+}/Ni) = -0.250 V_{SHE}
E^0 (Fe^{2+}/Fe) = -0.440 V_{SHE}
E^0 (Cr^{3+}/Cr) = -0.774 V_{SHE}

From Fig. 2 and Fig. 3, it seems that the tendency for PbO to act as an oxidizer on the surface of passive film of alloy 690 is grater in pH 10 solution than in pH 4 solution. Further, it is evident from Eq. (5) that the reaction between Cr and PbO is most thermodynamically to occur. This is presumably the reason for the polarization behavior of alloy 690 in pH 10 solution containing PbO (Fig. 1(b)), which demonstrates that PbO enhances the dissolution of Cr in the passive film.

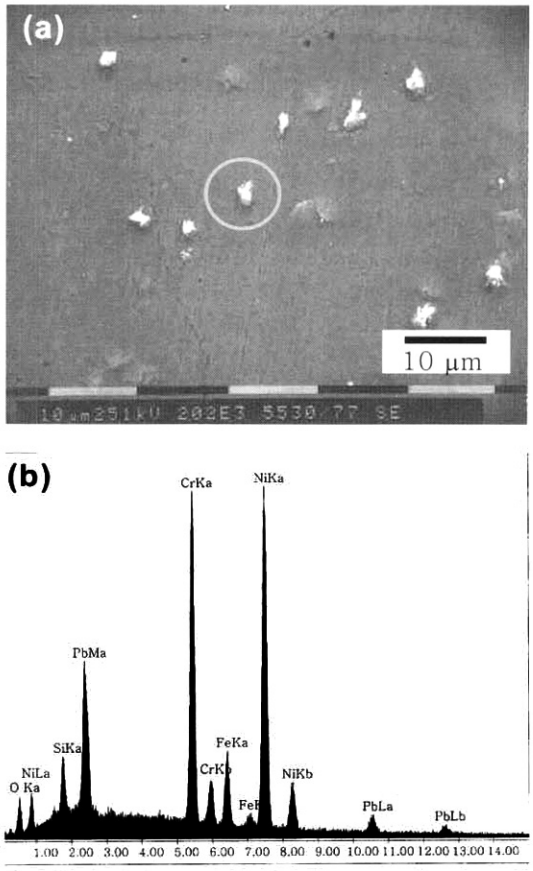

Fig. 2. SEM micrograph(a) of passive film formed in 90 ℃, pH 4 solution with 500 ppm of PbO at 100 mV_{SCE} for 2 hours. EDS result for the precipitate circled in (a) is shown in (b).

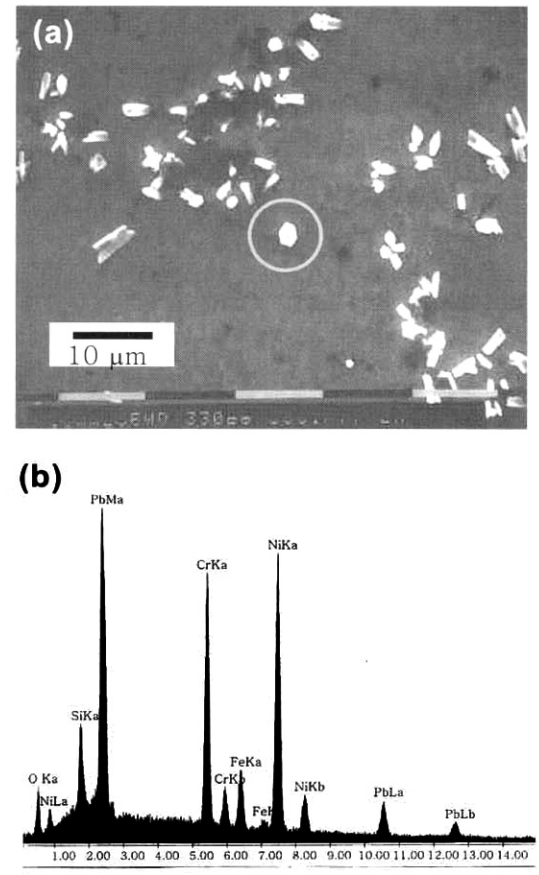

Fig. 3. SEM micrograph(a) of passive film formed in 90 ℃, pH 10 solution with 500 ppm of PbO at 100 mV_{SCE} for 2 hours. EDS result for the precipitate circled in (a) is shown in (b).

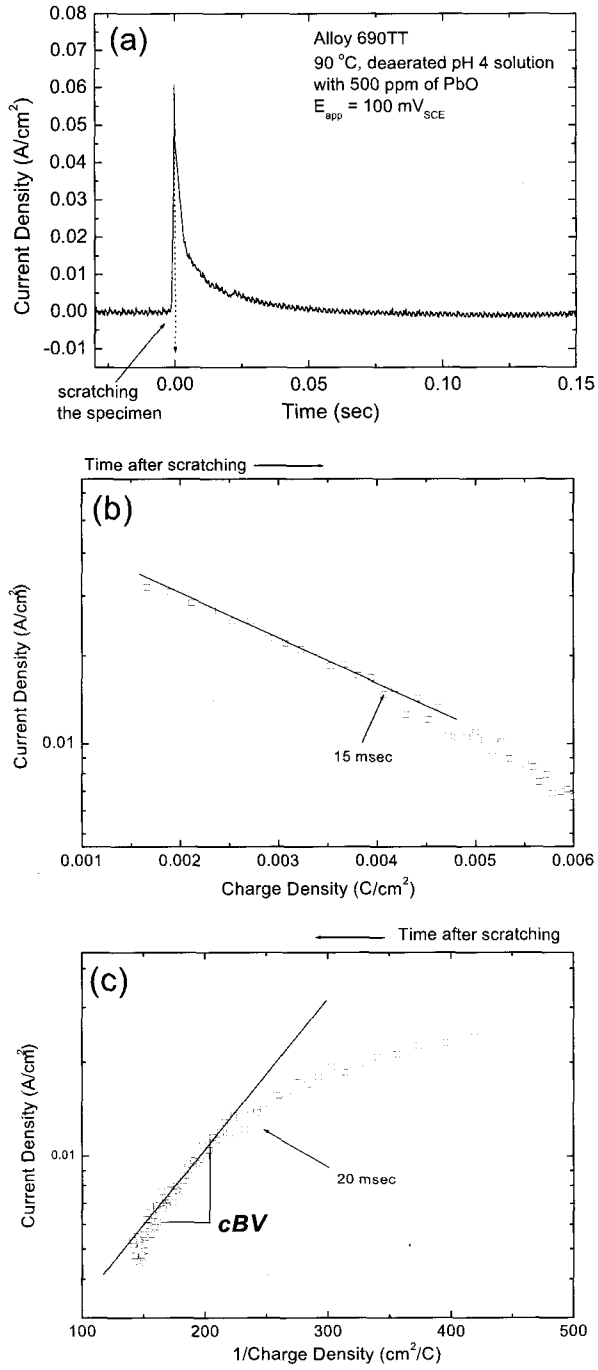

Fig. 4. (a) Current transient curve; (b) log i(t) vs. q(t); and (c) log I(t) vs. 1/q(t) plot of Alloy 690 in 90 °C, deaerated pH 4 solution with 500 ppm of PbO at the applied potential of 100 mV_{SCE}.

4.3 Repassivation kinetics of alloy 690

Fig. 4(a) shows a typical current transient curve for Alloy 690 when a scratch was made on the surface of the alloy polarized to a passive potential, 100 mV_{SCE} in 90 °C, deaerated pH 4 solution with 500 ppm of PbO. Once the passive film is broken by a scratch, the anodic current flowing from the scratch increases abruptly to a peak due to an anodic oxidation reaction, and thereafter decreases as repassivation proceeds. Based on the data in Fig. 4(a), the *log i(t) vs. q(t)* and the *log i(t) vs. 1/q(t)* plots were drawn respectively according to Eq. 1 and 4, and presented in Fig. 4(b) and (c). Evidently, the repassivation of Alloy 690 occurred in consecutive processes with different kinetics: passive film initially nucleated and grew for about 15 milliseconds according to the place exchange model, in which *log i(t)* was linearly proportional to *q(t)*, and thereafter grew according to the high field ion conduction model from 20 to 100 milliseconds, in which *log i(t)* was linearly proportional to *1/q(t)*. After 100 milliseconds, the anodic current density, *i(t)*, scattered over a small range of current density with a little increase in the charge density, *q(t)*, probably due to reaching a steady-state. In all solutions used in this study, current transient curves of alloy 690 exhibited repassivation behavior similar to that described above. The transition of film growth mechanism from the place exchange model to the high field ion conduction model appears to occur because the activation energy for the place exchange process of M-O pairs increases as the film grows, and then reaches to the value beyond which the place exchange process of M-O pairs can not occur. From this result, it was checked that the repassivation kinetics of alloy 690 can be explained by the two models and that the *cBV*, a parameter for repassivation rate and SCC susceptibility of stainless steels, can also be applied to alloy 690.

4.4 Effects of PbO on the repassivation kinetics

The current transient curves for alloy 690 in pH 4 and in pH 10 water were shown in Fig. 5(a) and in Fig. 6(a), respectively. In both solutions, the anodic current density of the alloy is clearly higher in solution with PbO than in solution without PbO. Kwon et al.[12] reported that the repassivation rate of an alloy can be compared by the repassivation time, t_r, that has been passed to achieve the predetermined degree of repassivation from scratching, a certain value of repassivation current, i_r. The shorter is the repassivation time, the faster will be the repassivation rate of an alloy. In Fig. 5(a) it takes shorter time for alloy 690 in PbO-free solution, t_r, to be repassivated to a predetermined degree of repassivation (i_r) than that, $t_{r,PbO}$, in PbO containing solution. Fig. 6(a) shows similar trends. Thus, it can be known that repassivation rate of alloy 690 decreased by addition of PbO to both solutions. The *log i(t) vs. 1/q(t)* plots were drawn in Fig. 5(b) and in Fig. 6(b) using the data of the current transient curves of Fig.

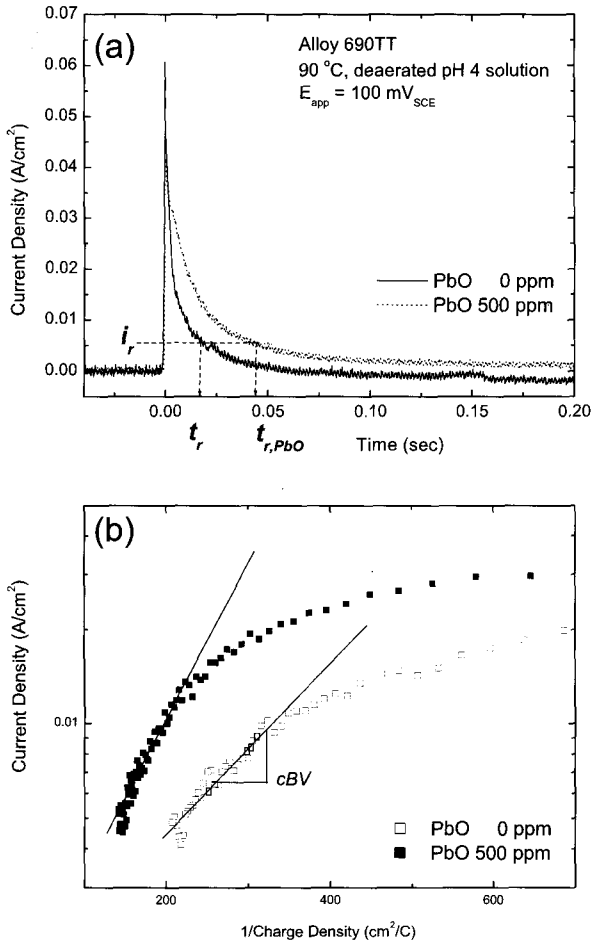

Fig. 5. (a) Current transient curves and (b) log i(t) vs. 1/q(t) plots of Alloy 690 in 90 ℃, deaerated pH 4 solution at the applied potential of 100 mV_{SCE}.

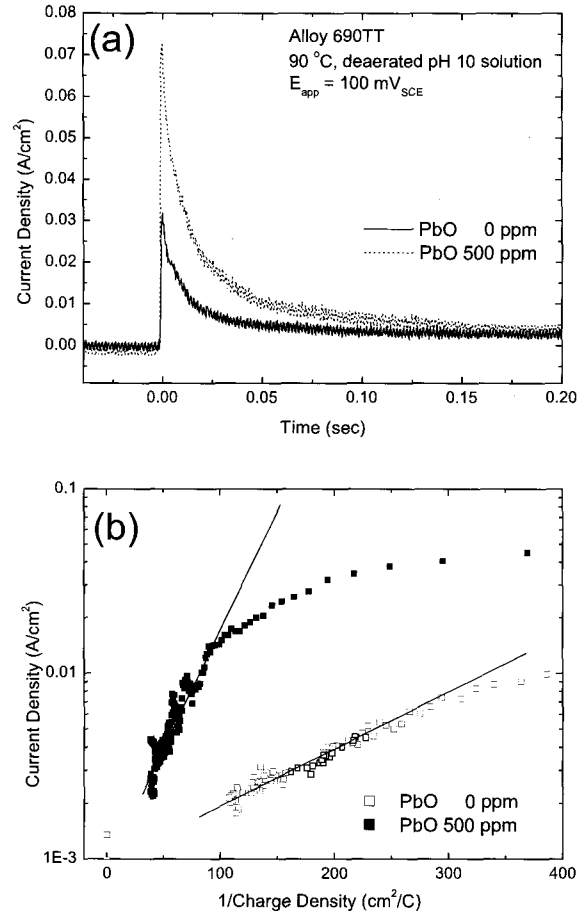

Fig. 6. (a) Current transient curves and (b) log i(t) vs. 1/q(t) plots of Alloy 690 in 90 ℃, deaerated pH 10 solution at the applied potential of 100 mV_{SCE}.

5(a) and Fig. 6(a), respectively. Evidently, the value of *cBV* is higher in both solutions containing PbO, which demonstrates that repassitvation rate of alloy 690 is slower and SCC resistance of that alloy is lower in PbO containing solution than in PbO free solution.

The change in the value of *cBV* with different PbO concentration in both solutions was shown in Fig. 7. As mentioned above, the value of *cBV* increased with PbO in both solutions, but the change of *cBV* was grater in pH 10 than in pH 4 solution. This result is well agreed with other researchers' reports that lead induced SCC of Ni-based alloy has been observed mainly in alkaline environments1.[6),17),18)] From this experimental result, the reason for the increase in SCC susceptibility of alloy 690 in solution contaminated with lead is due presumably to the decrease in repassivation rate of the alloy. To investigate any compositional or structural changes in passive film that caused the decrease in the repassivation rate of alloy 690 in solution with PbO, Mott-Schottky, AES and

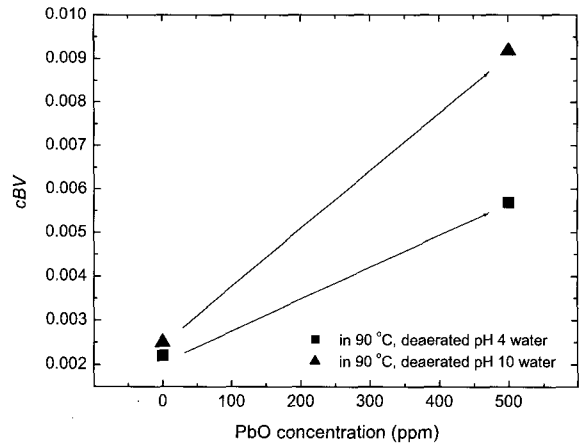

Fig. 7. Effect of PbO on the change in the value of cBV in 90 ℃, deaerated pH 4 and pH 10 solution at the applied potential of 100 mV_{SCE}.

XPS analyses on the passive film of the alloy were conducted.

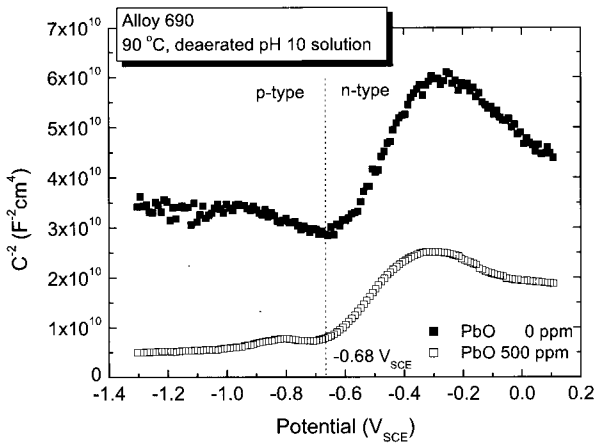

Fig. 8. Mott-Schottky plot of Alloy 690 obtained in 90 ℃, deaerated pH 10 solution at a frequency of 1000 Hz.

4.5 Effects of PbO on the semi-conducting properties of passive film on alloy 690

The electronic properties of passive film can be explored by measuring the capacitance of the space charge layer (C_{SC}) as a function of the electrode potential (U). The Mott-Schottky relationship expresses the potential dependence of C_{SC} of a semiconductor electrode under the depletion condition ;[19]

$$\frac{1}{C_{SC}^2}=\frac{2}{\varepsilon\varepsilon_O eN_D}\left(U-U_{FB}-\frac{kT}{e}\right) \quad \text{for n-type semiconductor (6)}$$

where e is electron charge, ε is the dielectric constant of the passive film, ε_o is the permittivity of free space (8.854 (10^{-14} Fcm^{-1}), N_D is the donor density, U_{FB} is the flat band potential, k is the Boltzman constant, and T is the absolute temperature. The value of U_{FB} can be determined from the extrapolation of the C_{SC}^{-2} vs. U plots to the U axis at C_{SC}^{-2} = 0. The Mott-Schottky relationship is based on the assumption that the capacitance of the space charge layer is much less than that of the Helmholtz layer.[20] Normally Helmholtz capacitance of 25 ~ 50 μFcm^{-2} satisfies this assumption.

Fig. 8 shows the effects of PbO on the Mott-Schottky plot for the passive film formed on alloy 690 grown at 100 mV_{SCE} in pH 10 solution for 2 hours at 90 ℃. The positive slope of the Mott-Schottky plots in the potential region above -0.68 V_{SCE} indicates that the passive film formed on alloy 690 is an n-type semiconductor in this potential region, whereas the passive film is a p-type semiconductor in the potential region below -0.68 V_{SCE} where the slopes are negative. M.D.C. Belo et al.[21] reported that in spite of higher Ni content in the alloy, the electronic properties of passive film on Alloy 690 was dominated by Cr oxide (p-type) and Fe oxide (n-type) through the capacitance measurement of alloy 600 in pH 9.2 buffer solution at room temperature. M. F. Mentemor et al.[22] reported that electronic properties of passive fulm on Alloy 690 also showed same behavior as that on alloy 600. Therefore, two semi-conducting types appeared in Fig. 8 is presumably due to Cr oxide (p-type) and Fe oxide (n-type). It should be noted here that Mott-Schottky behavior of passive film formed in PbO containing solution did not show marked p-type semi-conductivity. Considering that p-type semi-conductivity comes from Cr oxide in the passive film, there seems to be a decrease in Cr content in the passive film by PbO addition to the solution. To confirm the Cr depletion in the passive film, AES depth analysis for the film was conducted.

4.6 Effects of PbO on the composition of passive film on alloy 690

Film formation procedure for AES analysis was same with that for Mott-Schottky analysis. Fig. 9 shows AES depth profile of passive film formed on Alloy 690. Three major alloying elements (Ni, Cr, Fe) were normalized to 100 %. In Fig. 9, Cr depletion regions at the outer parts of the film were found for both samples whose film grown in pH 10 solution without(a) and with(b) PbO, respectively. Cr depletion was more significant and extended to longer depth for the passive film formed in PbO containing solution than that formed in PbO-free solution. This result is well consistent with that of Mott-Schottky analysis, suggesting a decrease in Cr content in the passive film by PbO addition to the solution. From Mott-Schottky and AES analyses, it can be concluded that the compositional changes in passive film that caused the decrease in the repassivation rate of Alloy 690 with PbO is the Cr depletion in the film.

4.7 XPS analysis of passive film on alloy 690

XPS analysis for the passive film was conducted to confirm the existence of Pb compounds in the passive film. Film formation procedure was same as that for AES and Mott-Schottky analyses. Fig. 10(a) shows wide scan results for the unsputtered samples. For the passive film of sample 1, which grown in PbO containing solution, Pb 4f X-ray peak appeared clearly at about 150 eV of binding energy. There was no Pb peak on the film grown in Pb-free solution, sample 1. It means there exist Pb components on the outermost surface of film or at least within it. Fig. 10(b) shows narrow scan results of Pb peaks for the sample 1 after being sputtered for 3 minutes. The sputtering rate was 2.5 Å/min calibrated for SiO_2. Although it is difficult

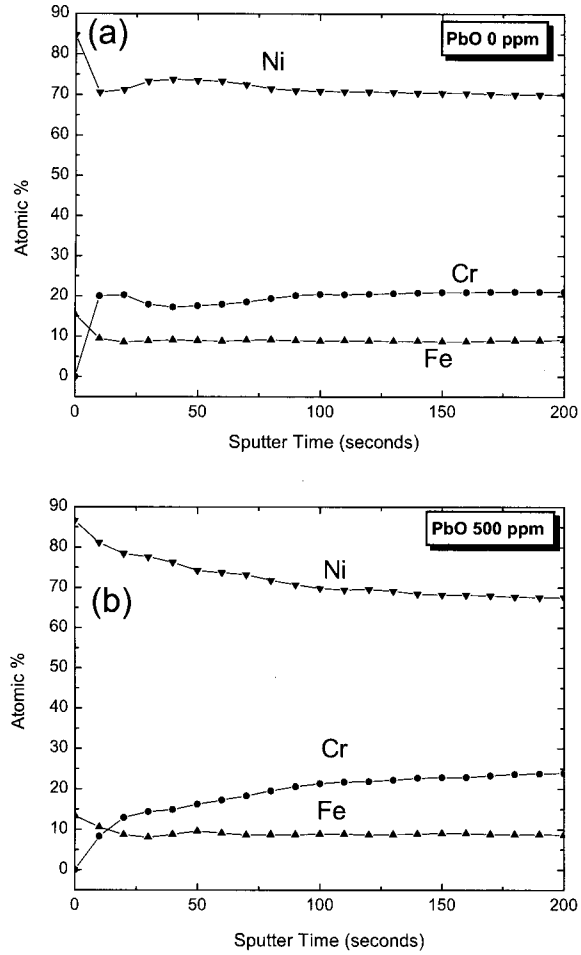

Fig. 9. AES depth profile of passive film on Alloy 690 in 90 ℃ pH 10 solution without(a) and with(b) PbO. (10 kV, 20 μm, take off angle 90 °, sputter rate : 1.6 Å /sec calibrated with SiO_2)

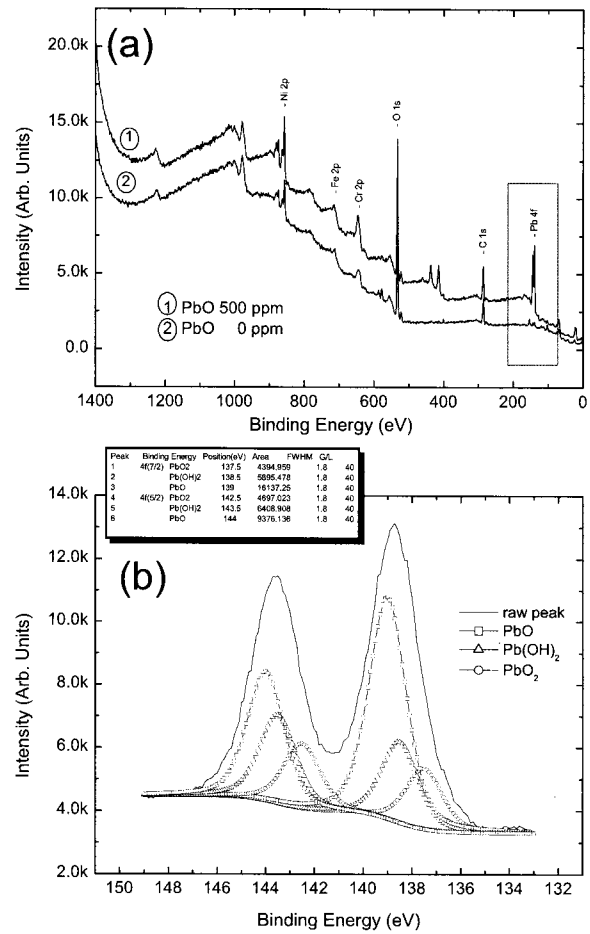

Fig. 10. (a) XPS wide scan result of unsputtered passive film formed in 90 ℃, pH 10 solution. (b) narrow scan spectra of Pb compounds after being sputtered for 3 minutes of the sample in (a) with a sputter rate of 2.5 Å /min calibrated with SiO_2. (Al-Kα, 15 kV 20 mA 300 W, take off angle : 90°)

to determine the chemical states of Pb compounds, for the overlap of various peaks of Pb compounds, it is clear that Pb compounds also exist in the inner parts of the passive film. Here the reaction mechanism of incorporation of Pb into the passive film is unclear. The reaction shown in Eq. 5 can not fully explain that and further research is needed.

5. Conclusions

1) It was confirmed from anodic polarization curve that the Cr trans-passive potential of alloy 690 was lowered by addition of PbO to the solution (328 mV_{SCE} → 249 mV_{SCE}).

2) Repassivation of alloy 690 occurred in two kinetically different processes; passive film initially nucleated and grew according to the place exchange model in which log *i(t)* is linearly proportional to *q(t)*, and then grew according to the high field ion conduction model in which log *i(t)* is linearly proportional to *1/q(t)* with a slope of *cBV*.

3) Addition of PbO to pH 4 and 10 solutions decreased the value of *cBV* of alloy 690, reflecting slower repassivation rate and higher SCC susceptibility of that alloy in solution with PbO than in solution without PbO. The increase in the value of *cBV* was grater in pH 10 than in pH 4 solution.

4) The increase in SCC susceptibility of alloy 690 with the addition of PbO to solution was presumably due to the Cr-depletion in the outer parts of passive film of the alloy with an incorporation of Pb compounds in the film, which was revealed by Mott-Schottky, AES and XPS analyses.

Ackowledgemetns

The authors acknowledge the financial support of Korea Institute of Nuclear Safety (KINS). This work was also partly supported by the Brain Korea 21 project.

References

1. A. K. Agrawal and J. P. N.Paine, *Proceedings of 4th Int'l Symposium on Environmental Degradation of Materials in Nuclear Power Systems - Water Reactor* -, p.7-1, Aug. 6-10, 1989, Jekyll Island, Georgia, NACE, Houston, USA (1990).
2. B. P. Miglin and J. M. Sarver, *Proceedings of 4th Int'l Symposium on Environmental Degradation of Materials in Nuclear Power Systems - Water Reactor* -, p.7-18, Aug. 6-10, 1989, Jekyll Island, Georgia, NACE, Houston, USA (1990).
3. B. P. Miglin and J. M. Sarver, *Proceedings of 5th Int'l Symposium on Environmental Degradation of Materials in Nuclear Power Systems - Water Reactor* -, p.757, Aug. 25-29, 1991, Monterey, California, ANS, La Grange park, USA (1992).
4. A. Rocher, F. Cattant, D. Buisine, B. Prieux, and M. Helie, *Proceedings of Contribution of Materials Investigation to the Resolution of Problems Encountered in PWRs*, p.537, Fontevraud III, 12-16, Sept. 1994, SFEN, France (1994).
5. J. M. Sarver, *Proceedings of 1987 EPRI Workshop on secondary - side intergranular corrosion mechanisms*, p.C11, vol.2 EPRI NP-5971, Sept., (1988).
6. F. Vaccaro, *Proceedings of 1987 EPRI Workshop on secondary - side intergranular corrosion mechanisms*, p.C12, vol.2 EPRI NP-5971, Sept., (1988).
7. T. Sakai, T. Senjuh, K. Aoki, T. shigemitsu, and Y. Kiahi, *Proceedings of 5th Int'l Symposium on Environmental Degradation of Materials in Nuclear Power Systems - Water Reactor* - p.764, Aug. 25-29, 1991. Monterey, California, ANS, La Grange park, USA (1992).
8. J. C. Scully, Environment Sensitive Fracture of Engineering Materials, Z.A. Foroulis (Ed.), p.71, AIME, New York, 1979.
9. N. Sato and M. Cohen, *J. Electrochem. Soc.*, **111**, 512 (1964).
10. N. Cabrera and N. F. Mott, *Rep. Prog. Phys.*, **12**, 163 (1948).
11. G. T. Burstein and P. I. Marshall, *Corros, Sci.* **23**, 125 (1983).
12. H. S. Kwon, E. A. Cho, and K. A. Yeom, *Corrosion*, **56**, 32 (2000).
13. E. A. Cho, C. K. Kim, S. J. Kim, and H. S. Kwon, *Electrochim. Acta*, **45**, 1933 (2000).
14. K. H. Lee, G. Cragnolino, and D. D. Macdonald, *Corrosion*, **41**, 540 (1985).
15. D. Feron, I. Lambert, *Proceedings of 12th Int'l conference on properties of water and steam.*-, Sept. 12-15, Orlando, FL, U.S.A. (1994).
16. M. Helie, I. Lambert, and G. Santarini, *Proceedings of 7th Int'l Symposium on Environmental Degradation of Materials in Nuclear Power Systems - Water Reactor* -, p.247, Aug. 7-10, Breckenridge, Colorado, NACE, Houston, 1995.
17. R. W. Staehle, *Proceedings of 1st Int'l conference on Environmental - Induced Cracking of Metals*, Kohler, WI, USA, Oct. 2-7, NACE, Houston, 1990.
18. A. M. Lancha, M. Garcia, M. Gernandez, *Proceedings of Int'l conference on Chemistry in Water Reactor*, Nice, Frace, April. 24-27, 1994.
19. J. F. Dewald, *J. Phys. Chem. Solid*, **14**, 155 (1960)
20. R. De Gryse, W. P. Gomes, F. Cardon, and J. Vennik, *J. Electrochem. Soc.*, **122**, 711 (1975)
21. M. D. C. Belo, N. E. Hakiki, and M. G. S. Ferreira, *Electrochim. Acta*, **44**, 2473 (1999).
22. M. F. Montemor, M. G. S. Ferreira, N. E. Hakiki, and M. D. C. Belo, *Corros. Sci.*, **42**, 1635 (2000).